

## SUPPLEMENTAL MATERIALS AND METHODS

### ***Materials***

Sphingosine-1-phosphate (S1P) was purchased from Biomol (Hamburg, Germany), JTE013 from Tocris Bioscience (Ellsville, USA) and tumour necrosis factor  $\alpha$  (TNF $\alpha$ ) from Sigma-Aldrich (St. Louis, USA). The MOPS-buffered salt solution contained [mmol/L]: NaCl 145, KCl 4.7, CaCl<sub>2</sub> 3.0, MgSO<sub>4</sub> •7H<sub>2</sub>O 1.17, NaH<sub>2</sub>PO<sub>4</sub> •2H<sub>2</sub>O 1.2, pyruvate 2.0, EDTA 0.02, MOPS (3-morpholinopropanesulfonic acid) 3.0, and glucose 5.0. Phosphate-buffered saline contained [mmol/L] 150 NaCl, 1.6 K<sub>2</sub>HPO<sub>4</sub>, 0.4 KH<sub>2</sub>PO<sub>4</sub>, 0.7 CaCl<sub>2</sub>, 1 MgSO<sub>4</sub> and 5.0 glucose. Culture medium was composed of Leibovitz L-15 base medium supplemented with 15% fetal calf serum (FCS), 0.4 $\mu$ mol/L L-glutamine, 20000U/L penicillin and 20mg/L streptomycin. All buffer and culture medium components were purchased from Sigma-Aldrich. The plasmids encoding the sphingosine kinase 1 (Sk1) constructs (Sk1<sup>G82D</sup>, Sk1<sup>S225A</sup>, Sk1-GFP) have been previously described<sup>1,2</sup>. The TB2-Sk1 construct was prepared using site-directed mutagenesis as previously described<sup>3</sup> and confirmed by sequencing. Ketamine (Ketavet®; Parke-Davis, Berlin, Germany) and Xylazine (Rompun®; Bayer, Leverkusen, Germany) were used to anesthetize guinea pigs for intravital microscopy experiments.

### ***Experimental Procedures***

This investigation conforms to the *Guide for the Care and Use of Laboratory Animals* published by the US National Institutes of Health (NIH Publication No. 85-23, revised 1996). All experimental protocols complied with Canadian, American and German federal animal protection laws and were approved by the Institutional Animal Care and Use Committees at The University of Toronto, Toronto, Canada; Kansas State University, Manhattan, USA; and Ludwig-Maximilians University, Munich, Germany.

### ***Intravital fluorescence microscopy of the cochlear microcirculation***

The guinea pig cochlear window preparation has been described previously<sup>4</sup>. Male albino Hartley guinea pigs (250-400g) that were anesthetized with i.p. injections of Ketamine/Xylazine (initial dose of 85mg/kg / 8.5mg/kg and supplemented 42.5mg/kg / 4.25mg/kg every 45 minutes thereafter). The core body temperature of anesthetized animals was kept at 38 $\pm$ 1°C using a thermostatically controlled heating pad. A left femoral artery polyethylene catheter (PE50) served to monitor systemic blood pressure and obtain blood sample for arterial blood gas and serum electrolyte evaluation; intravenous injections were applied through a right external jugular

vein catheter. Heart rate and pulse oxygenation of the spontaneously breathing animals were continuously monitored.

The mastoid bulla was exposed and removed through a postauricular approach to the right ear. To provide better access to the cochlea, the tympanic membrane, the posterior annulus, and the tensor tympani tendon were cut and all middle ear ossicles sacrificed. Mucosa and mucosal vessels overlying the second and the third cochlear turns were gently wiped off by a piece of gel foam. A small rectangular window (0.2 x 0.3 mm in size) was cut over the convex part of the second turn and a small intact piece of bone was removed from the cochlea. The cochlear bony wall was elevated without traumatizing the underlying spiral ligament and stria vascularis to expose blood vessels in these tissues.

Intravital microscopy was performed using a modified Zeiss microscope (Axiotech Vario; Zeiss, Goettingen, Germany) and intravenously injected fluorescein isothiocyanate (FITC)-labelled dextran (MW 500,000; 0.05-0.1 ml of a 5% solution in 9% NaCl) to visualize the cochlear microcirculation. FITC was excited by epi-illumination (100 W mercury lamp) and observed via specific fluorescence filter blocks (excitation 450-490 nm, emission  $\geq 515$  nm). The area of interest within the cochlear window was magnified using a long distance 20x objective (Olympus SLMPlan). Images were acquired using a SIT video camera (C2400-08; Hamamatsu, Herrsching, Germany) and digitally recorded (AY-DV124AMQ; Panasonic, NJ, USA) for subsequent off-line analysis of vessel diameter and blood flow (Cap Image analysis system; Zeintl, Heidelberg, Germany). For each treatment group (i.e.,  $\text{TNF}\alpha$  and  $\text{TNF}\alpha + \text{JTE013}$ ), parameters were analyzed using a total of 6 capillaries from 3 guinea pigs.

#### ***In vitro measurements of capillary diameter***

The isolation of gerbil spiral ligament capillary beds has been previously described<sup>5</sup>. Gerbils were euthanized and then decapitated. The temporal bones were removed from the head and opened. The spiral ligament was dissected from the cochlea and the *stria vascularis* was removed. The isolated spiral ligament was transferred to a bath chamber as a flat sheet, where it was then continuously superfused with PBS (2.5 bath volumes exchanged each second).

Because direct measurement of capillary diameter yields a poor signal-to-noise ratio, an indirect method, based on the measurement of red blood cell (RBC) movement with the capillary lumen, was utilized. RBCs trapped within the capillary lumen are perfect markers for luminal fluid

volume, since they do not stick to or disturb the vessel wall. Movement of luminal fluid and hence, RBCs, occurs in response to diameter changes and/or transendothelial fluid flux. Thus, under iso-osmotic conditions, the velocity of marker RBCs is a correlate measure of the vascular diameter. The precise model relating RBC movement to diameter is well-defined and has been described in detail previously <sup>5,6</sup>.

Isolated capillaries were occluded on one end, opened on the other end, and RBCs trapped inside the lumen were visualized by laser-scanning microscopy (510 Meta, Carl Zeiss, Göttingen, Germany). The capillary lumen between the occluded end the RBC was assumed to be a cylinder of constant volume that undergoes proportional changes in diameter and length during vasoconstriction. The length of the capillary was determined using a hyperosmotic step (300-337mosM) that drives a defined water-flux across the capillary wall and is experimentally observed as RBCs travelling toward the occluder. Vasoconstriction elicits movement of RBCs towards the open end of the capillary.

A combined tracing illustrating RBC displacement following S1P stimulation is provided in Supplemental Figure 1. Representative time-lapse movies displaying capillary vasomotor responses are also provided as “**Movie 1 - osmotic step.gif**” and “**Movie 2 - S1P.gif**”

#### ***In vitro measurements of vascular tone in the spiral modiolar artery***

The isolation of the spiral modiolar artery (SMA) has been previously described in detail <sup>7,8</sup>. Gerbils were euthanized and then decapitated. The temporal bones were removed from the head, opened and placed in micro-dissection chamber containing ice-cold MOPS buffer. The otic capsule enclosing the cochlea was opened and the bone surrounding the modiolus was removed. The SMA was then gently removed from the eighth cranial nerve, taking care not to stretch the artery. Once isolated, the SMA was cut into ~1.5mm segments, cannulated and pressured hydrostatically to 30cmH<sub>2</sub>O. The vessel segments were maintained in culture medium for 24 hours, with continuous perfusion (culture medium) at a rate of 0.5ml/h. Transfection of genetic constructs (Sk1<sup>G82D</sup>, Sk1<sup>S225A</sup>, Sk1-GFP) <sup>1,2</sup> was completed during the 24 hour vessel culture period using Effectene® reagent (Qiagen; Hilden, Germany), according to the manufacturer's instructions.

All functional experiments were performed at 37°C in MOPS buffer, as previously described <sup>8</sup>. SMA viability was confirmed by testing its vasoconstrictor response to 3mmol/L Ca<sup>2+</sup> under depolarizing conditions (125mmol/L KCl). All values of tone represent acute diameter

measurements that have been normalized: the values represent the magnitude of vessel constriction relative to maximal diameter. The computation of tone is as follows:  $\text{tone (\% of dia}_{\text{max}}) = (\text{dia}_{\text{max}} - \text{dia}_{\text{measured}}) / \text{dia}_{\text{max}} \times 100$ . The apparent  $\text{Ca}^{2+}$  sensitivity of the contractile apparatus was assessed as the relationship between microvascular tone and intracellular  $\text{Ca}^{2+}$  levels. Intracellular  $\text{Ca}^{2+}$  levels were adjusted by increasing extracellular  $\text{Ca}^{2+}$  ( $\text{Ca}^{2+}_{\text{ex}}$ ) from 0 to 10mmol/L under depolarizing conditions (120mmol/L  $\text{K}^{+}$ ).

We have observed that the baseline level of calcium sensitivity can significantly fluctuate in separate batches of animals. We cannot explain why this occurs, however, the animal-to-animal variability within a batch of animals is generally quite consistent, which allows for clear statistical results with only 5-6 experiments per group. All experiments were therefore designed as paired experiments (i.e., pre/post-treatment) or, in the case of transfection experiments, all treatment groups within an experimental series were completed with the same batch of animals. Statistical comparisons across different experimental series were avoided.

***Description of human subjects included in etanercept treatment study***

The use of human subjects in this study conforms with the principles outlined in the Declaration of Helsinki <sup>9</sup> and was approved by the Human Studies Ethics Committee of the Technische Universität München; Munich, Germany (#2172/08).

A total of 12 adult patients presenting with the typical symptoms of SHL (with or without vertigo and/or symptoms of uni-/bi-lateral Meniere's disease) were identified and selected for treatment. As an inclusion requirement, patients showed either no or only a partial response to a conventional prednisolone treatment regime [high-dose, 500 mg/day i.v., for three days, followed by 16 days of weaning (starting at 100mg p.o. daily with 20mg dose reduction every 2 days and a further reduction to 10, 5, and 2.5mg/day)]. Patient exclusion criteria included: the presence of an underlying infection; a history of acute, chronic or recurrent serious infections; inadequate cardiac, pulmonary, renal or hepatic function; neurological disorders; elevated red blood cell count or C-reactive protein; and/or a history of malignancy. Female patients who were pregnant or breast-feeding were also excluded; non-menopausal female patients were required to use birth control for the duration of etanercept treatment.

Prior to enrolment, we obtained informed written consent for the off-label use of etanercept. Each patient's cardiac, hepatic and renal functions were specifically assessed, as well as his/her overall health status, documented through an interview, physical examination, chest radiography, magnetic resonance imaging (MRI) of the brain and determination of several laboratory parameters (erythrocyte sedimentation rate (ESR), HsP70, white blood cell count, C-reactive protein (CRP), serum aspartate aminotransferase levels, syphilis serology, serum creatinine levels, glucose levels, antineutrophil cytoplasmic antibodies (ANCA) and antinuclear antibodies (ANA). Other medications for the treatment of symptoms caused by Meniere's disease (e.g., diuretics and sedatives) were halted for the duration of the study, as their actions could confound the results. Etanercept was self-administered subcutaneously twice a week for 12 weeks (25 mg; similar to the dose routinely used for the treatment of rheumatoid arthritis).

A composite of the patients included in the study is provided in Supplemental Table 1. A total of 19 ears (from 12 patients) with hearing loss were monitored; these were subcategorized into 9 cases of "acute" (symptoms <3 months) and 10 cases of "chronic" (symptoms present for >3 months) hearing loss, depending on when treatment for the condition was sought. Two patients reported adverse reactions to etanercept (neither patient displayed auditory improvement before discontinuation of treatment): the exclusion of their cases from data analysis reduced the respective pools to 8 acute and 7 chronic cases (i.e., 1 acute and 3 chronic hearing loss cases were excluded).

In 8 patients, 6 acute and 2 chronic cases of hearing loss was associated with systemic inflammatory diseases (i.e., rheumatoid arthritis, inflammatory bowel diseases, ankylosing spondylitis, diabetes mellitus type I, non-alcoholic fatty liver disease (NAFLD) and autoimmune hepatitis); non-immune mediated cochleovestibular disease (non-IMCVD), indicated by otologic symptoms, appeared to be the primary etiology in the other 5 patients. Five of the 12 patients presented with "unilateral" hearing loss (i.e., only in one ear). Patients with acute hearing loss (symptoms occurred for less than 3 months; 8 treated ears in 7 patients) were analyzed separately from those where the symptoms had become chronic (prevalent for more than 3 months; 7 treated ears in 5 patients), since permanent structural alterations in hearing transduction (i.e., death of sensory hair cells) may have occurred by this time. Our analysis excludes 2 patients that discontinued treatment due to adverse reactions.

Hearing function was assessed by pure-tone audiometry, speech reception threshold and word recognition. Pure-tone average (PTA) was performed from 9 frequencies between 250 and 6000Hz (250, 500, 750, 1000, 1500, 2000, 3000, 4000, and 6000Hz). Measurements were taken at 1, 2, 3, 4, 8, and 12 weeks post-initiation of etanercept treatment. Improvement of hearing was defined as an improvement of (i) sensorineural hearing from baseline (ii)  $\geq 20$  dB in the pure-tone air conduction thresholds in at least 3 of the tested frequencies and (iii) 15 dB at 2 consecutive frequencies.

## SUPPLEMENTAL RESULTS

### *Specificity of JTE013*

We have previously demonstrated that JTE013 inhibits S1P-stimulated vasoconstriction in the SMA and hamster resistance arteries <sup>10</sup>. However, demonstrating that JTE013 specifically inhibits S1P<sub>2</sub> receptor-dependent responses in the SMA is rather difficult, because only two agents have been documented to evoke vasoconstriction in un-branched SMA segments (which we use in our experimental setup) to date: endothelin-1 (ET-1) and S1P. Although ET-1 stimulates SMA vasoconstriction, a portion of the response appears to be dependent on S1P (i.e., ET-1 stimulates S1P synthesis and consequently S1P<sub>2</sub> receptor dependent signaling pathways; unpublished observations): thus, ET-1 responses in the SMA could be partially inhibited by JTE013. In support of these observations, ET-1-dependent activation of Sk1 in smooth muscle cells has been demonstrated previously by others <sup>11</sup>.

As an alternate means of assessing JTE013 specificity, we assessed the effect of JTE013 on norepinephrine responses in isolated hamster gracilis muscle resistance arteries <sup>12</sup>. We used a norepinephrine concentration of 0.3 $\mu$ M, which elicits a sub-maximal constriction of the hamster resistance artery. We found no effect of JTE013 (pre-JTE013: 37 $\pm$ 3%; post-JTE013: 38 $\pm$ 2%; n=6 paired observations, P>0.05). We acknowledge that this control experiment was conducted using a different species and a vessel from a different vascular bed; however, in conjunction with our previous evidence that JTE013 inhibits S1P-dependent vasoconstriction in the same artery <sup>10</sup>, this control experiment provides an indication that JTE013 is acting specifically at the 1 $\mu$ mol/L concentration.

## SUPPLEMENTAL FIGURES

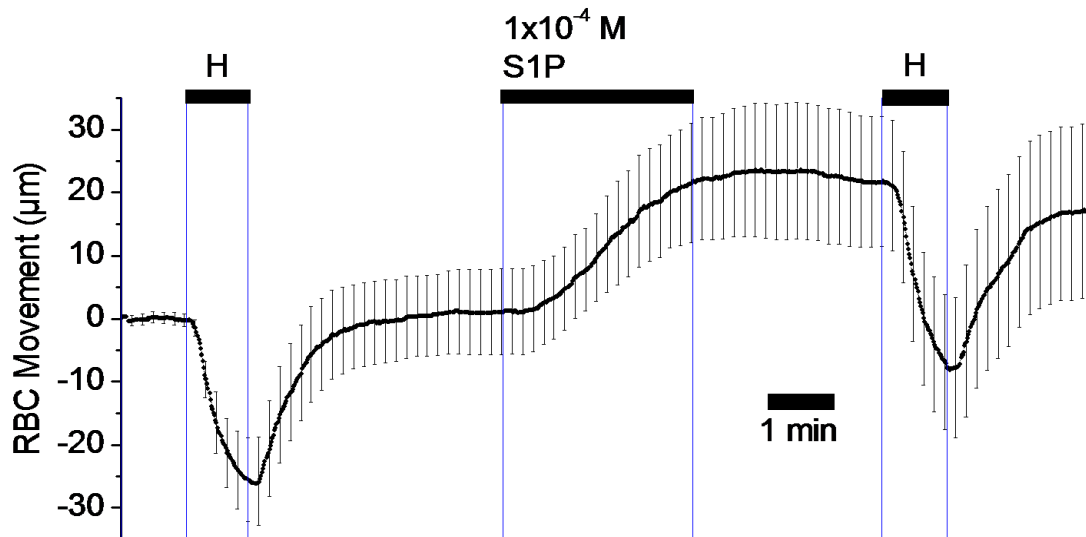
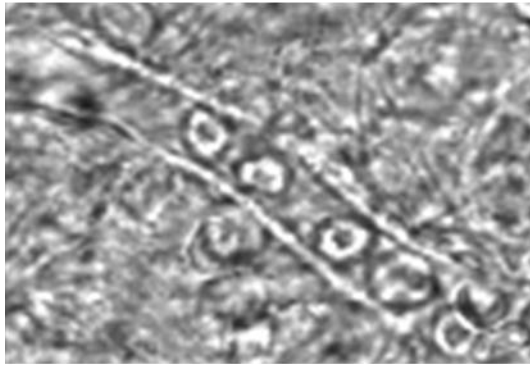


**Figure 1: S1P stimulates a change in capillary diameter in spiral ligament capillaries**

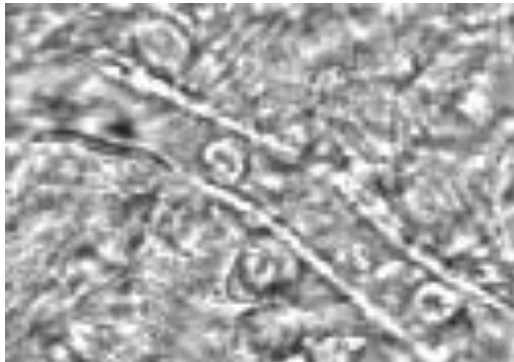
Shown are combined tracings (mean $\pm$ SEM; n=9) of normalized red blood cell (RBC) displacements, a correlate of capillary diameter, in response to a hyperosmotic step (from 300 to 337 mosM; marked by “H”) and 100 $\mu$ mol/L S1P. Measurements were made in 1s intervals; error bars are given every 10s. The marker RBC moved toward the occluder when a water efflux was induced by the hyperosmotic challenge. In contrast, the marker RBC moved toward the open end, when the capillary constricted in response to S1P.



**File: Osmotic step.gif**

**Movie 1: Laser-scanning microscopy of a capillary in the isolated spiral ligament: response to osmotic step.**

The capillary was occluded on the left side and open on the right side. Increasing the osmolarity from 300 to 337 mosM caused movement of RBCs toward the occluder. Restoring the osmolarity from 337 to 300 mosM caused a similar movement of the RBCs to the open end. The original length of this sequence is 120 sec.



**File: S1P.gif**

**Movie 2: Laser-scanning microscopy of a capillary in the isolated spiral ligament: response to S1P.**

The capillary was occluded on the left side and open on the right side. Addition of 100 $\mu$ mol/L sphingosine-1-phosphate (S1P) caused visible constriction of the capillary and movement of RBCs toward the open end. The original length of this sequence is 290 sec.



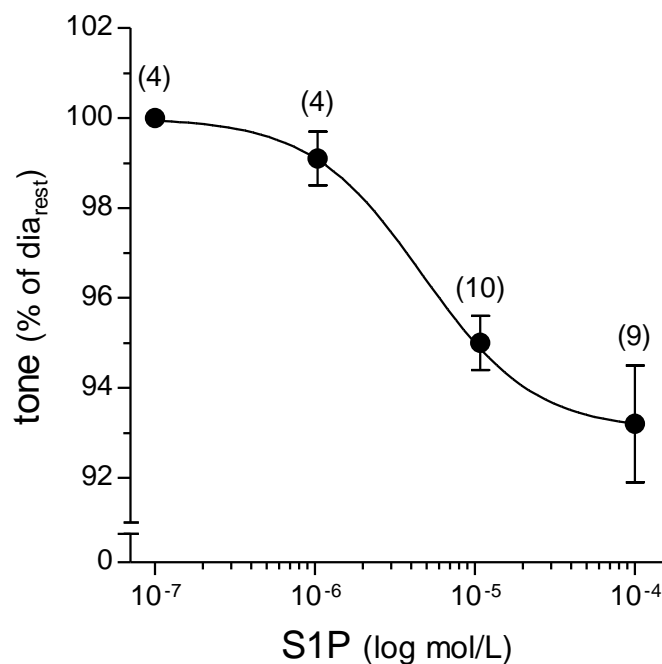


**Figure 2: S1P stimulates dose-dependent vasoconstriction of spiral ligament capillaries**

S1P-stimulated reductions in capillary diameter were measured in an *ex vivo* preparation of capillary beds isolated from the spiral ligament of the cochlear lateral wall. The number of capillaries measured for each S1P concentration is indicated in parentheses. Using a sigmoid curve to fit the 4 data points, the EC<sub>50</sub> was approximated to be 4.7 μmol/L.

**SUPPLEMENTAL TABLE**

	sex age	Hearing loss	Improvement during treatment (week 1-12)	Background diseases	ANCA ANA ds-DNS	Notes
1	♀ 56	AHL, right ear	CR	Non-alcoholic fatty liver disease (NAFLD)	- - -	
2	♀ 42	AHL, right ear CVD	CR	Diabetes mellitus Type I	- -/+ -	Etanercept improved insulin resistance
3	♀ 36	AHL, right ear	CR	-	- - -	Discontinued because of pregnancy after 14 days of treatment. CR within this time
4	♂ 36	AHL, right ear	PR	Steatosis hepatitis	- - -	
5	♀ 31	AHL, both ears CVD	CR left ear PR right ear	Auto-immune hepatitis	+ + -	
6	♂ 57	AHL, left ear CVD	NI	immune-mediated CVD	- + +	
7	♀ 46	AHL, left ear CHL, right ear CVD	PR, left ear (acute) NI, right ear (chronic)	-	- - -	AHL recovered completely within 1 year. CHL never improved.
8	♂ 42	CHL, both ears	PR	HLA B27 assoc.; initial ankylosing spondylitis	- + -	Last hearing loss progression occurred more than a year prior to current treatment
9	♀ 32	CHL, both ears	NI	-	- - -	
10	♂ 48	CHL, both ears CVD	NI	-	- - -	
11	♀ 25	CHL, both ears CVD	NI after 2 weeks, treatment discontinued because of AR	Colitis ulcerosa	- - -	AR: rash at injection site
12	♀ 82	AHL, left ear CHL, right ear	NI after 1 week, treatment discontinued because of AR	Hypothyroidism; Rheumatoid arthritis; RF: +	- + -	AR: rash at injection site & headache.

**Table 1. Demographic characteristics of patients treated with etanercept**

Patients had a mean age of  $44.4 \pm 4.6$  years. Involvement describes if patients had one or both ears affected. Acute hearing loss (AHL) was defined as a hearing loss that happened less than 3 months prior to enrolment. Otherwise hearing loss was termed chronic (CHL). Cochleovestibular disease was assumed in patients that had objectifiable signs of vestibular affection in addition to hearing loss.

**Abbreviations:** AR = Adverse Reactions; CR = Complete remission; PR = Partial remission; NI = No improvement; CVD = Cochleovestibular disorder; ANCA = Antineutrophil cytoplasmic antibody; ANA = antinuclear antibody, ds-DNS = anti-dsDNA antibodies; RF = Rheumatoid factor.

## SUPPLEMENTAL REFERENCES

1. Pitson SM, Moretti PA, Zebol JR, Xia P, Gamble JR, Vadas MA, D'Andrea RJ, Wattenberg BW. Expression of a catalytically inactive sphingosine kinase mutant blocks agonist-induced sphingosine kinase activation. A dominant-negative sphingosine kinase. *J Biol Chem*. 2000;275:33945-33950.
2. Pitson SM, Xia P, Leclercq TM, Moretti PA, Zebol JR, Lynn HE, Wattenberg BW, Vadas MA. Phosphorylation-dependent translocation of sphingosine kinase to the plasma membrane drives its oncogenic signalling. *J Exp Med*. 2005;201:49-54.
3. Xia P, Wang L, Moretti PA, Albanese N, Chai F, Pitson SM, D'Andrea RJ, Gamble JR, Vadas MA. Sphingosine kinase interacts with TRAF2 and dissects tumor necrosis factor- $\alpha$  signaling. *J Biol Chem*. 2002;277:7996-8003.
4. Canis M, Arpornchayanon W, Messmer C, Suckfuell M, Olzowy B, Strieth S. An animal model for the analysis of cochlear blood flow disturbance and hearing threshold in vivo. *Eur Arch Otorhinolaryngol*. 2010;267:197-203.
5. Wangemann P, Liu J. Osmotic water permeability of capillaries from the isolated spiral ligament: new in-vitro techniques for the study of vascular permeability and diameter. *Hear Res*. 1996;95:49-56.
6. Sadanaga M, Liu J, Wangemann P. Endothelin-A receptors mediate vasoconstriction of capillaries in the spiral ligament. *Hear Res*. 1997;112:106-114.
7. Wangemann P, Gruber DD. The isolated in vitro perfused spiral modiolar artery: pressure dependence of vasoconstriction. *Hear Res*. 1998;115:113-118.
8. Scherer EQ, Lidington D, Oestreicher E, Arnold W, Pohl U, Bolz SS. Sphingosine-1-phosphate modulates spiral modiolar artery tone: A potential role in vascular-based inner ear pathologies? *Cardiovasc Res*. 2006;70:79-87.
9. World Medical Association Declaration of Helsinki. Recommendations guiding physicians in biomedical research involving human subjects. *Cardiovasc Res*. 1997;35:2-3.
10. Kono M, Belyantseva IA, Skoura A, Frolenkov GI, Starost MF, Dreier JL, Lidington D, Bolz SS, Friedman TB, Hla T, Proia RL. Deafness and stria vascularis defects in S1P2 receptor-null mice. *J Biol Chem*. 2007;282:10690-10696.
11. Leiber D, Banno Y, Tanfin Z. Exogenous sphingosine 1-phosphate and sphingosine kinase activated by endothelin-1 induced myometrial contraction through differential mechanisms. *Am J Physiol Cell Physiol*. 2007;292:C240-C250.
12. Lidington D, Peter BF, Meissner A, Kroetsch JT, Pitson SM, Pohl U, Bolz SS. The phosphorylation motif at serine 225 governs the localization and function of sphingosine kinase 1 in resistance arteries. *Arterioscler Thromb Vasc Biol*. 2009;29:1916-1922.